0273-2289/03/105-108/0471/$20.00

Effects of Pressure Pulsation on Oxygen Transfer Rate Measured by Sulfite Method

Wei-Cho Huang,* Cheng S. Gong, and George T. Tsao

School of Chemical Engineering, Purdue University, West Lafayette, IN 47907-1283; E-mail: huangwc@che.eng.ohio-state.edu

Abstract

Pressure pulsation (PP) was investigated for its effects on oxygen transfer rate (OTR) measured by sulfite oxidation. By manipulating airflow rate, 0.41–1.2 vvm, and a control valve in a 4-L bioreactor, the frequency of PP was varied at different gas pressures3–15 psig. A mathematical model of OTR was built and compared to experimental data. OTR was also examined at constant gas pressure, 4.5–15.0 psig. The results indicate a good agreement between measurement and model prediction. OTR above 9 psig during PP showed significant enhancement at 25°C. This proves that PP not only affects the elevation of DO level, but also increases the interfacial area and mass transfer coefficient.

Index Entries: Oxygen transfer; pressure pulsation; sulfite oxidation.

Introduction

Oxygen limitation is a long-term problem in aerobic fermentation or cell culture, because oxygen has low solubility in water. Dissolved oxygen (DO) concentration is generally kept as high as possible by increasing the oxygen transfer rate (OTR) to support aerobic processes. High agitation and/or airflow rate is the most commonly used strategy to improve OTR *(1,2)*. There are also some studies on the effects of DO *(3)* and periodic changes in pressure on the bioprocess *(4–6)*. In recent years, the techniques of pressure pulsation (PP) *(7)* and oscillating dissolved oxygen tension *(8)* have been applied to biologic systems, to enhance OTR or DO level in fermenting liquid to produce more desired product (metabolite).

Our previous report showed increased productivity and yield of glycerol in highly aerobic yeast fermentation by about 6.8 and 26%, respectively *(7)*, owing to enhanced OTR resulting from PP. The OTR was not affected by gas flow rate above the loading point. To evaluate quantitatively the effect of PP on OTR, a sulfite oxidation method was applied to measure OTR at different peak pressure, p_m, and cycle, t_2, (reciprocal of frequency)

*Author to whom all correspondence and reprint requests should be addressed.

of PP, respectively. A mathematical model for oxygen transfer was derived from the equation of OTR with the resistance of liquid film as the rate-limiting step. The model includes considerations of various physical phenomena involved in oxygen transfer. By maintaining gas at a different constant pressure, the measured OTR was compared with that calculated from the model.

Materials and Methods

Pressure Pulsation

PP is achieved by placing an on-off valve at the gas outlet of an enclosed reactor *(7)*. When the exit valve is closed ($t = 0$), the pressure in the vessel will build up owing to the accumulation of inflow; when the exit valve is open ($t = t_1$), the vessel depressurizes to atmospheric pressure at the end of each cycle ($t = t_2$). This pressurization and depressurization, repeated periodically, is called PP.

A 6-L New Brunswick glass, stirred bioreactor was used in this study involving sulfite oxidation. By changing the aeration rate from 0.41 to 1.2 vvm, but fixing each cycle ($t_1 = 24$ s, $t_2 = 30$ s), one can bring pressure in the enclosed fermentor to pulsate at different p_ms (mean pressure) between 3 and 15 psig. By changing different cycles t_2 between 15 and 50 s, but keeping the aeration rate from 0.63 to 1.3 vvm, and also $t_1/t_2 = 4/5$, one can bring different frequencies of PP at the same p_m, 9 psig. By adjusting inlet flow and holding outlet flow between 0.93 and 1.1 vvm, one can achieve the condition of different fixed pressures, from 4.5 to 15 psig. Further details are discussed next.

Oxygen Transfer Rate

The liquid film, surrounding the gas bubbles, is usually the rate-limiting step for oxygen transfer from gas bubbles to cells owing to low solubility of oxygen in aqueous solutions *(9)*. The rate of oxygen transfer *(10)* from the gas to liquid phase is given by

$$\mathrm{OTR} = \frac{dC_L}{dt} = k_L a \left(C^* - C_L\right)$$

in which k_L is the oxygen transfer coefficient, a is the gas-liquid interfacial area, C^* is the saturated DO concentration, and C_L is the actual DO concentration in the broth.

Measurement of Sulfite Oxidation

In the presence of Cu^{2+} as a catalyst, sulfite is oxidized to sulfate in a zero-order reaction *(11)*. Because of the rapid reaction, the actual DO concentration in the broth approaches zero. The OTR is the same as the rate of oxygen consumption, which is half the rate of sulfate formation.

In a 6-L fermentor, 4 L of 0.2 mol/L Na_2SO_3 and 6.7 mL of 0.63 mol/L $CuSO_4$ solutions were added. Under different peak pressures, cycles of PP,

Table 1
Effect of Different PPs on OTR Measured by Sulfite Oxidation[a]

p_m[b] (psig)	Aeration rate (vvm)	OTR[c]	SE
No	1.0	2.5E-03	1.4E-04
3	0.41	2.4E-03	2.5E-04
6	0.65	2.5E-03	1.4E-04
9	0.88	2.8E-03	5.4E-05
12	1.1	3.1E-03	2.5E-04
15	1.2	3.2E-03	2.4E-04

[a]Same cycle of PP was kept at t_1 = 24 s and t_2 = 30 s.
[b]p_m = peak pressure of PP.
[c]OTR (M/min) was measured at 25°C with a working volume of 4 L.

or constant pressures, described before, OTR was studied at 25°C. A 5-mL sample of sulfite solution taken from the fermentor at different intervals was mixed with 5 mL of 0.2 *N* KI-I_2 solution. Excess I_2 was titrated with the 0.1 mol/L standard thiosulfate ($Na_2S_2O_3$) solution. The rate of the molar change of $Na_2S_2O_3$ solution used for the titration of two consecutive samples equals the fourth of the OTR.

Results

Effect of Different PPs on OTR

OTR with different PPs (same cycle, t_2 = 30 s) was measured three times for each set of experimental conditions at 25°C. Table 1 shows that a higher peak pressure of PP can reach a faster OTR. OTR with 15 psig of PP was about 35% faster than that with 3 psig of PP. OTR without PP was about 5% faster than that with 3 psig of PP and was close to that with 6 psig of PP. Since k_L is related to airflow rate below loading point *(12)*, OTR with an aeration rate below 0.65 vvm or 3 psig will be a function of aeration rate. OTR decreased by lowering gas flow rate has a greater effect than that increased by higher p_m. Nevertheless, this does not affect the result of our mathematical model. The model was derived, as shown subsequently, from OTR based on unit gas volume in the dispersion.

Effect of Different PP Cycles on OTR

The OTRs at various PP cycles were determined in triplicate at 25°C (*see* Table 2). Generally, if a longer PP cycle (lower frequency) was applied, the measurement of sulfite oxidation gave a lower OTR. For example, the OTR with a 15-s PP cycle was 43% larger than that with a 50-s PP cycle. With a higher frequency of PP, there was more frequent, quick expansion of gas bubbles during the depressurization phase, which would create more fresh bubble surface area. According to Danckwerts's *(13)* surface renewal model, a freshly formed surface allows much faster interfacial mass transfer rates including OTR.

Table 2
Effect of Different PP Cycles
on OTR Measured by Sulfite Oxidation[a]

Cycle, t_2[b] (s)	Aeration rate (vvm)	OTR[c]	SE
15	1.3	3.4E-3	1.9E-04
20	1.2	3.1E-3	2.0E-04
25	1.1	3.0E-3	2.8E-05
30	0.88	2.8E-3	5.4E-05
35	0.82	2.8E-3	1.5E-04
40	0.74	2.6E-3	1.1E-04
50	0.63	2.4E-3	2.3E-04

[a]Same peak pressure, p_m = 9 psig, was applied.
[b]Where $t_1/t_2 = 4/5$.
[c]OTR (M/min) measured at 25°C with a working volume of 4 L.

Table 3
Effect of Different Constant Pressures
on OTR Measured by Sulfite Oxidation

P (psig)	Aeration rate (vvm)	OTR[a]	SE
4.5	0.93	2.7E-03	1.7E-04
9	1.1	3.1E-03	1.9E-04
12	1.1	3.3E-03	1.7E-04
15	1.0	3.3E-03	1.7E-04

[a]OTR (M/min) measured at 25°C with a working volume of 4 L.

Effect of Different Constant Pressures on OTR

The effect of different PPs was compared with OTR measured at constant pressure that was selected to equal the time-integrated average pressure during a PP cycle. The OTRs at different constant pressures were measured in triplicate runs at 25°C. Table 3 shows that increasing gas pressure increased the OTR owing to the higher solubility of oxygen in the broth, according to Henry's law. The OTR with 9 psig of PP in Table 1 is 4% higher than that of the corresponding time-integrated average pressure of 4.5 psig. However, the OTR at the 50-s PP cycle in Table 2 is 13% lower than that at a constant pressure of 4.5 psig. The main reason should be that the aeration rate, 0.63 vvm, under the 50-s PP cycle was below the gas-loading point. This is similar to the situation when the OTRs with 3 psig of PP were smaller than that without PP.

Discussion

Mathematical Model of OTR (Effects of PP)

Our studies were conducted at different average gas flow rates. Changing the volumetric flow rate did not change the inlet pressure, but the

pressure dropped across the sparger nozzle. This also changed the size of bubbles and the gas flow rate throughout the pulsation. However, assuming no coalescence of bubbles, the number of bubbles was the same owing to the proportionality between the size of the bubbles and the gas flow rate. Thus, it is reasonable to take an average of the size of the bubbles and assume that the number of bubbles was the same throughout the pulsation for mathematical modeling.

During the pressurization phase, the bubbles had longer residence time owing to the smaller radius of the bubbles; by contrast, the bubbles flew upward rapidly during the depressurization phase. However, we kept the ratio of the period from the pressurization to the depressurization phase the same. In other words, the effect of bubble residence time should not be different in our studies.

The total surface area and volume of bubbles inside the fermentor are written respectively as

$$A = n(4\pi r^2) \tag{1}$$

$$V = n(4/\ 3\pi r^3) \tag{2}$$

in which n is the total number of bubbles, and r is the assumed average radius of bubbles.

Then by dividing Eq. 1 by Eq. 2, the gas-liquid interfacial area, a, is defined as follows:

$$a = A/V = 3/r \tag{3}$$

Assuming the gas in the dispersion obeys the idea gas law,

$$pV = K \tag{4}$$

in which K is a constant.

From Eq. 2 and 4, assuming no coalescence of bubbles, so that n is a constant, and taking the reciprocal of radius, then

$$1/r = Bp^{1/3} \tag{5}$$

in which B, a constant, is defined as $[4n\pi\ /(3K)]^{1/3}$.

Substituting Eq. 5 into Eq. 3, and taking the first-order time derivative of interfacial area, a,

$$a = 3Bp^{1/3} \tag{6}$$

$$da/dt = Bp^{-2/3}dp/dt \tag{7}$$

Applying Henry's law ($HC^* = p$) and taking the first-order time derivative of saturated DO concentration, C^*,

$$C^* = pH^{-1} \tag{8}$$

$$dC^*/dt = H^{-1}dp/dt \tag{9}$$

Meanwhile, the pressure change inside the fermentor by PP can be approximated as linear functions for each cycle of the pressurization phase (interval t from zero to t_1) and the depressurization phase (interval t from t_1 to t_2), respectively:

$$p_1 = (p_m/t_1)t + p_a \tag{10}$$

$$p_2 = (p_m/[t_1 - t_2])t + (t_2/[t_2 - t_1])p_m + p_a \tag{11}$$

in which p_1 and p_2 are the pressure inside the fermentor during the pressurization and depressurization phase, respectively; p_m is the peak pressure of PP; and p_a is the atmospheric pressure.

For the fast reaction, such as sulfite oxidation, $C_L = 0$, the OTR equation is simplified and differentiated as

$$d(\mathrm{OTR})/dt = k_L\left(da/dtC^* + adC^*/dt\right) \tag{12}$$

Substituting Eqs. 6–9 into Eq. 12, then

$$d(\mathrm{OTR})/dt = kp^{1/3}\, da/dt \tag{13}$$

$$\mathrm{OTR} = \tfrac{3}{4}kp^{4/3} + I \tag{14}$$

in which constant k is defined as $4k_LBH^{-1}$, and I is an integrating constant.

From Eqs. 10, 11, and 14, the OTR equation can be written as

$$\mathrm{OTR}_1 = \tfrac{3}{4}k\left([p_m/t_1]t + p_a\right)^{4/3} + I \tag{15}$$

$$\mathrm{OTR}_2 = \tfrac{3}{4}k\left([p_m/\{t_1 - t_2\}]t + [t_2/\{t_2 - t_1\}]p_m + p_a\right)^{4/3} + I \tag{16}$$

in which OTR_1 and OTR_2 are the OTRs during the pressurization and depressurization phase, respectively.

For each PP cycle, the time-integrated average OTR can be given from the integration of Eqs. 15 and 16,

$$\mathrm{OTR}_{avg} = \left(\int_0^{t_1} \mathrm{OTR}_1 dt + \int_{t_1}^{t_2} \mathrm{OTR}_2 dt\right)/t_2 \tag{17}$$

$$\mathrm{OTR}_{avg} = \frac{9k}{28p_m}\left([p_m + p_a]^{7/3} - {p_a}^{7/3}\right) + I \tag{18}$$

If Danckwerts's *(13)* surface renewal model is satisfied, Eq. 18 can be written as

$$\mathrm{OTR}_{avg} = MT_2^{-0.5}p_m^{-1}\left([p_m + p_a]^{7/3} - {p_a}^{7/3}\right) + I \tag{19}$$

in which $M = 9{D_1}^{0.5}B/7H$; and $D_1 = t_2{k_L}^2/60$, modified diffusion coefficient.

Model Fitting

The model of OTRs with different PPs, p_m = 3–15 psig (same cycle, 30 s), was fitted with nonlinear regression provided by Flying Raichu's

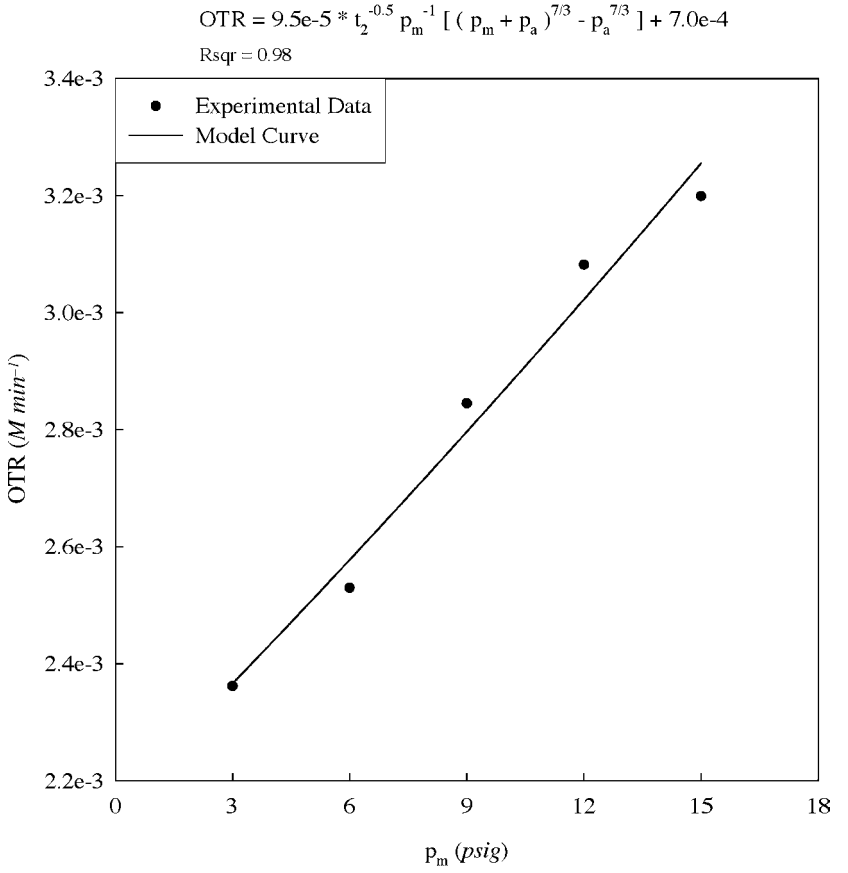

Fig. 1. Model of OTR with different PPs and same cycle, t_2 = 30 s.

SigmaPlot 2000 ver 6.10 (SPSS Science). Assuming that Danckwerts's *(13)* model is obeyed, the experimental data in Fig. 1 show good agreement with the model curve from Eq. 19 (M = 9.5e-5, I = 7.0e-4, *Rsqr* = 0.98, in which *Rsqr* = 1.0 if 100% matching).

In the case of different PP cycles, t_2 = 15–50 s, fitting with the same computer program and assumption, the result of fitting also gave good agreement between experimental data and the model curve (M = 7.0e-5, I = 1.3e-3, and *Rsqr* = 0.97; *see* Fig. 2). However the parameter M was 26% smaller, and I was 46% larger than that estimated from different PPs. This can be caused by deviation from the assumptions of ideal gas law, uniformity of the bubbles' size, and/or Danckwerts's *(13)* model.

Danckwerts's *(13)* model was checked by applying the parameters M and I computed from the model with different PPs, as shown in Fig. 3. The fitted power of t_2 is –0.50 and *Rsqr* is 0.85, which should be reasonable enough. However, some assumptions may need to be modified to get a better fit.

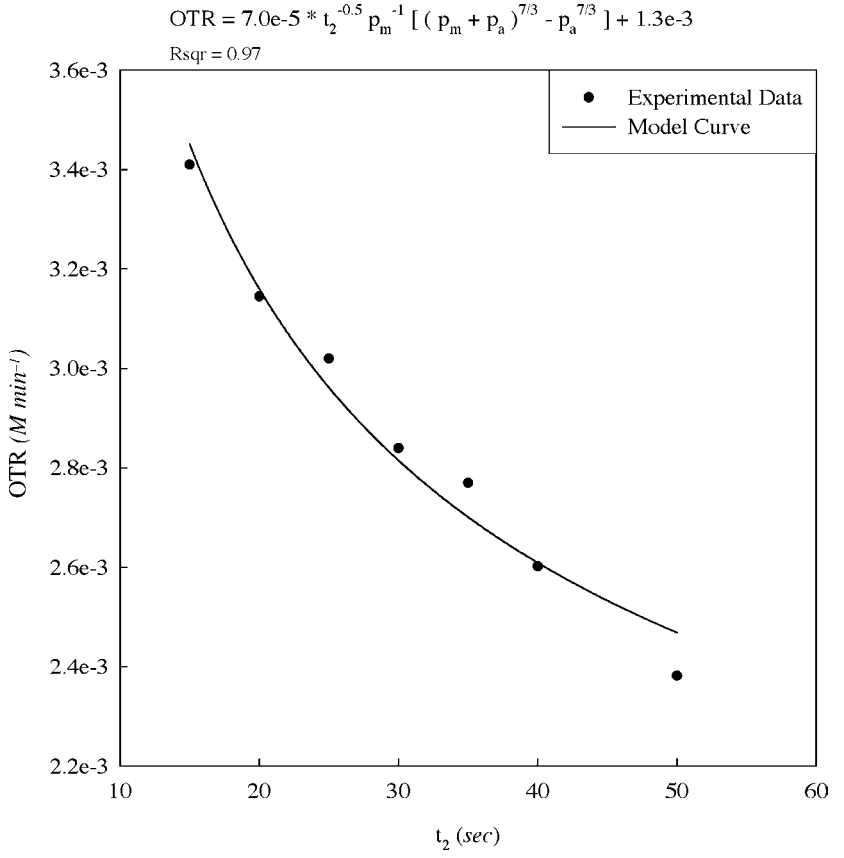

Fig. 2. Model of OTR with different cycles and same PP, p_m = 9 psig.

The OTR above 9 psig of PP showed significantly more enhancement than that above the corresponding fixed time-integrated average pressure of 4.5 psig (*see* Fig. 4). It is obvious that the OTRs above 9 psig of constant pressure showed a similar shape of saturation curve. By contrast, the experimental data and model curve of different PPs has the trend to rise linearly. Equation 7 gave the ratio of the bubble surface area change to the hydrostatic pressure change. This ratio was smaller if we elevated the pressure drop. Namely, the bubbles' area change was less important than the mass transfer coefficient at higher pressures of PP. The surface renewable dominated in this case. This proves that PP not only affects the elevation of DO level by higher pressure, but also increases the interfacial area and mass transfer coefficient by different PP cycles.

Conclusion

The OTR increased with peak pressure or frequency of PP. During the depressurization phase, it created more fresh bubble surface area with

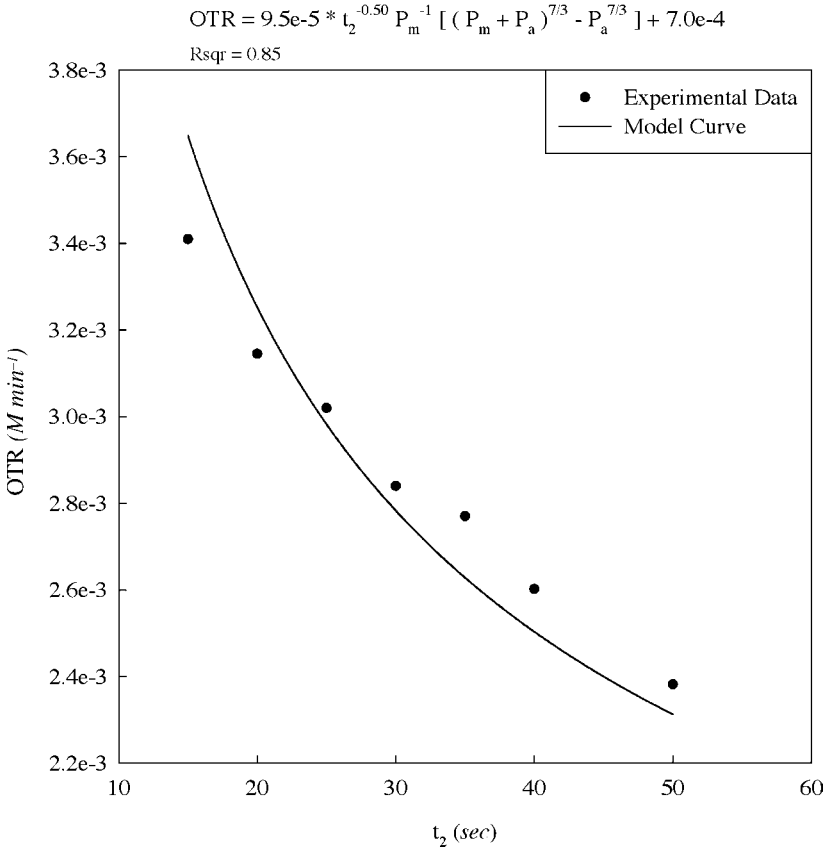

Fig. 3. Model of OTR with different cycles and same PP, p_m = 9 psig, by applying parameters *M* and *I* from Fig. 1.

higher peak pressure. From the surface renewal model, fresh interfacial area had a much higher rate of oxygen transfer than the old bubble surface area. In addition, the higher frequency of PP created a higher level of turbulence next to the bubble surface, which enhanced the value of k_L by increasing the frequency of surface renewal. Our studies indicated that a good agreement of measurement and theoretical model was achieved, and that the OTR above 9 psig of PP showed significantly more enhancement than that above the corresponding time-integrated average pressure at 25°C. Futhermore, keeping the aeration rate above the loading point can provide better improvement of OTR by PP.

Acknowledgments

We acknowledge the assistance provided by Tom Huang for the design of the fermentor. This research was supported in part by a grant from the National Science Foundation.

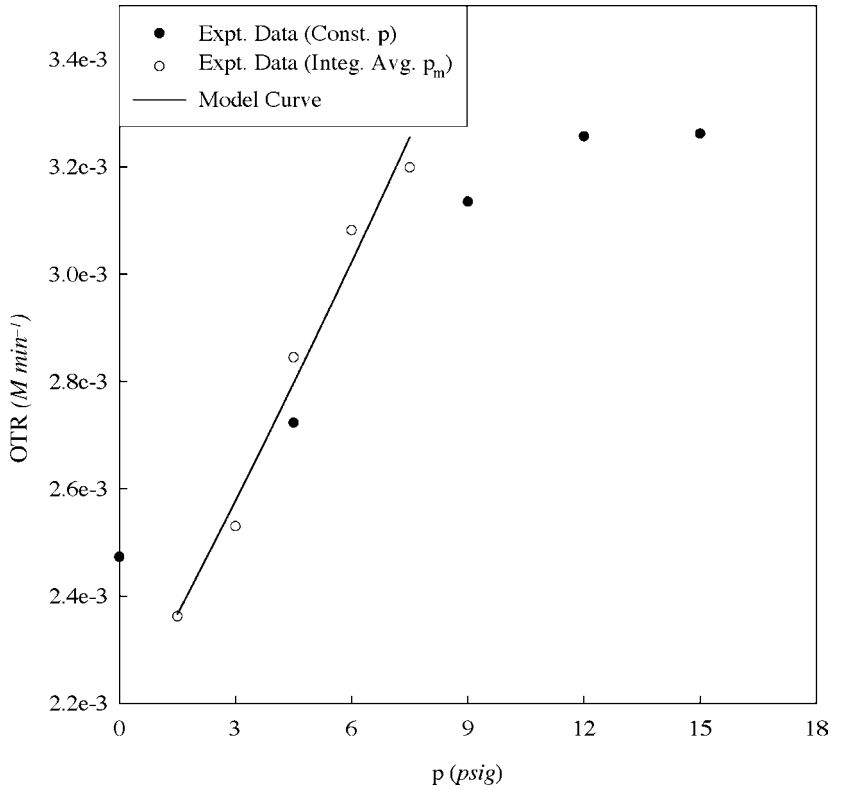

Fig. 4. Comparison of OTRs, different PPs, and constant pressures.

References

1. Finn, R. K. (1954), *Bacteriol. Rev.* **18,** 254–274.
2. Hixson, A. W. and Gaden, E. L. Jr. (1950), *Ind. Eng. Chem.* **42,** 1792–1801.
3. Kilburn, D. G. and Webb, F. C. (1968), *Biotechnol. Bioeng.* **10,** 801–814.
4. Kataoka, H., Sato, S., Mukataka, S., et al. (1986), *Biotechnol. Bioeng.* 28, 663–667.
5. Trager, M., Qazi, G. N., Buse, R., and Onken, U. (1992), *J. Ferment. Bioeng.* **74,** 282–287.
6. Rhiel, M. and Murhammer, D. W. (1995), *Biotechnol. Bioeng.* **47,** 640–650.
7. Huang, W.-C., Gong, C. S., and Tsao, G. T. (2002), *Appl. Biochem. Biotechnol.* **98–100,** 909–920.
8. Trujillo-Roldan, M. A., Pena, C., Ramirez, O. T., and Galindo, E. (2001), *Biotechnol. Prog.* **17,** 1042–1048.
9. Yoshida, F., Ikeda, A., Imakawa, S., and Miura, Y. (1960), *Ind. Eng. Chem.* **52,** 435–438.
10. Shuler, M. L. and Kargi, F. (1992), *Bioprocess Engineering*, Prentice Hall, Englewood Cliffs, NJ, p. 165.
11. Schultz, J. S. and Gaden, E. L. Jr. (1956), *Ind. Eng. Chem.* **48,** 2209–2212.
12. Cooper, C. M., Fernstrom, G. A., and Miller, S. A. (1944), *Ind. Eng. Chem.* **36,** 504–509.
13. Danckwerts, P. V. (1951), *Ind. Eng. Chem.* **43,** 1460–1467.